

SYDNEY HARBOUR: SEICHES, TIDES AND MEAN CIRCULATION

BRIAN PETRIE*

*Ocean and Ecosystems Sciences Division,
Fisheries and Oceans Canada
Bedford Institute of Oceanography, Dartmouth, NS B2Y 4A2*

ABSTRACT

Beginning with observations from 1901, sea level elevations and currents from Sydney Harbour are examined across a broad frequency range. The mean currents, annual components of sea level, tides and seiches, mainly in the South Arm, are the focus. Tidal and mean currents are $\sim 0.01 \text{ m s}^{-1}$. The general circulation is estuarine-like with a thin, near-surface outflow layer and a thicker, deeper inflow. The distribution of contaminants in bottom sediments suggests the circulation, though weak, plays a retentive role in the Arm, transporting sediments towards its head. Analysis of 11-years of sea level data indicates a strong annual cycle, more energetic during winter than from late spring to early fall. The increased energy occurred at all frequencies except for tides. Seiches, with periods of ~ 0.5 to 2 h, emerge as a strong contributor to sea level and currents. The distributions of elevation and flow amplitudes associated with seiches were derived. With maximum observed values of 0.74 m and 0.24 m s^{-1} , seiche displacements and currents can exceed those associated with tides and the mean circulation. While earlier studies identified only the dominant fundamental seiche mode, recent sea level data sampled at 1-minute show that modes 2-4 occur.

Keywords: Sydney Harbour, sea level, mean circulation, tides, seiches

INTRODUCTION

Sydney Harbour situated in eastern Cape Breton, Nova Scotia, opens onto Sydney Bight, the area of ocean bordered by Cabot Strait, Laurentian Channel and the eastern Scotian Shelf. The Harbour is 'Y' shaped with the seaward arm dividing into a Northwest and South Arm (Fig 1A, B). The South Arm is about 10 km long, 1 km wide and 10 m deep. Sydney River empties into the Harbour at its head and has an estimated peak monthly inflow of about $21 \text{ m}^3 \text{ s}^{-1}$ in April and a minimum inflow of about $5 \text{ m}^3 \text{ s}^{-1}$ in July and August (Gregory *et al.* 1993). At the annual average rate of $10.4 \text{ m}^3 \text{ s}^{-1}$,

* Author to whom correspondence should be addressed: petriebd@gmail.com

the freshwater inflow would take ~ 116 days to fill the South Arm. The South Arm of the Harbour is the focus of this study.

Several physical oceanographic studies have been carried out in Sydney Harbour over the past century. W. Bell Dawson, Superintendent of the Tidal and Current Survey of Canada, initiated a comprehensive program to establish reference benchmarks and collect sea level data for the Gulf of St. Lawrence and Atlantic Canadian ports, including Sydney, in the late 1800s (Dawson 1917; see Appendix, Fig A1). Dawson (1917) reported extreme low and high-water levels from continuously recording gauges placed in the Harbour at Battery Point in 1901 (July) and 1915 (July-October; see Fig 1A for location). Honda and Dawson (1911) analyzed the 1901 records for oscillations due to seiches, harmonic motions related to the

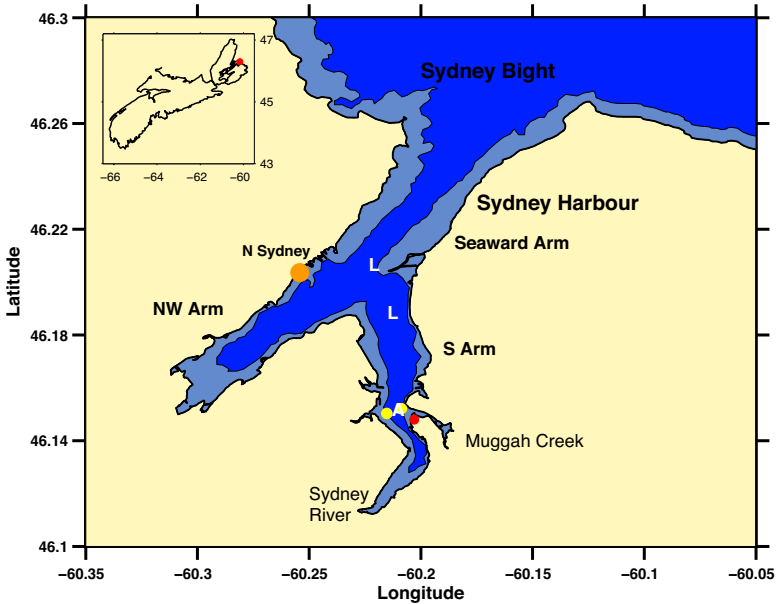


Fig 1A Map of Sydney Harbour opening onto the Sydney Bight to the northeast. The locations of the long-term tide gauge at North Sydney (large orange dot) and Sydney River, the main source of freshwater to the Harbour are indicated. The letters indicate the locations of current meter moorings by Lane (L; 1989, 1991) and ASA (A; 1994; off Muggah Creek); the 2 yellow dots, the sites of the Fisheries and Oceans ADCPs, 2000-2001 (off Muggah Creek). The red dot at the mouth of Muggah Creek marks Battery Point, the site of Dawson's tide gauge. Depths greater (shallower) than 10 m are shown in dark (light) blue. The inset shows the location of Sydney Harbour (red dot) relative to Nova Scotia.

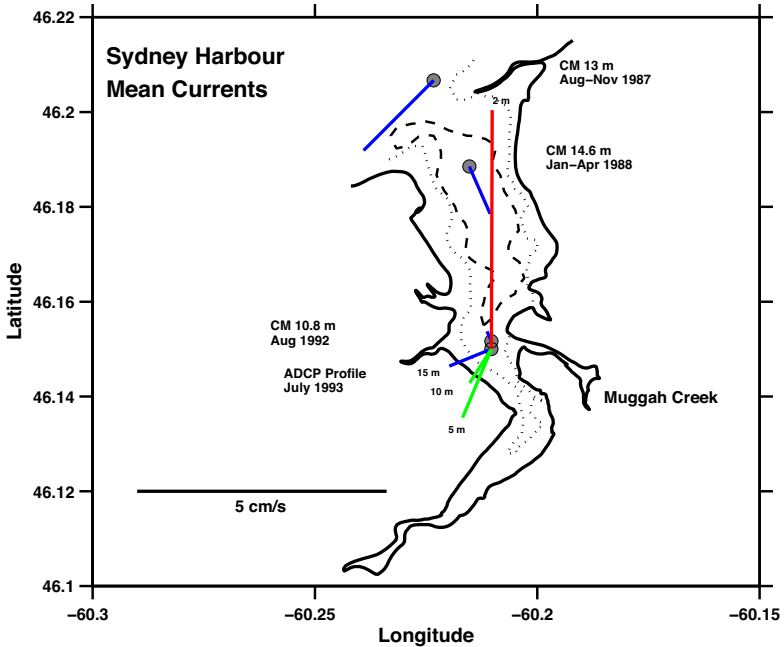


Fig 1B Bathymetry of the South Arm of Sydney Harbour showing the 10 m (dotted line) and 15 m isobaths (dashed line). Mean current vectors from the Lane and ASA moorings are shown. Blue, green and red vectors depict the current for depths > 10 m, 5-10 m and < 5 m. CM refers to single depth instruments. The current scale is indicated in the lower left of the figure.

geometry of an inlet. These resonances can limit the usefulness of many harbours and are generally most prominent as the fundamental mode (Miles and Munk, 1961). The period of the fundamental mode of a harbour of length L and depth z_0 is given by Merian's formula as $4L/(gz_0)^{1/2}$, where g is the acceleration due to gravity. Honda and Dawson (1911) calculated two dominant seiche periods of 120 and 132 minutes based on the dimensions of the Harbour from the mouth to the head of the Northwest and South Arms, respectively, and by assuming that the oscillations were generated independently in each arm. Easton (1972) refined the calculations of Honda and Dawson (1911) by constructing an analytical solution for a three-channel model of the Harbour with seaward, south and northwest arms. In addition, he developed a cross-sectionally averaged numerical model of the inlet. Easton (1972) reported a period of 124 minutes for the fundamental mode, close to the results of Honda and

Dawson (1911); he identified 3 additional, higher frequency modes. Some additional notes on these models are given in the Appendix.

Lane (1989, 1991) and ASA (1994) conducted environmental studies primarily in the South Arm. While the programs focused on pollutants in Harbour waters, in situ observations of currents (moored instruments, locations shown in Fig 1), temperature and salinity complemented the chemical sampling. The ASA (1994) program was related to the feasibility of developing a sewage treatment plant with effluent flowing into the Harbour. Supporting data included moored current meters (location shown in Fig 1, one single point instrument, 1 acoustic Doppler current profiler (ADCP) sampling at 1 m resolution from ~2 to 14 m, bottom depth 15 m), transects with ship-borne acoustic Doppler current profilers and hydrographic sampling (temperature and salinity). The currents derived from these moorings feature outflow from the South Arm concentrated in the near-surface (~0-2.5 m) with a deeper, more extensive inflow towards Sydney River (Fig 1B). Some of these data were used by Petrie *et al.* (2001) in a review of limited aspects of the physical oceanography of Sydney Harbour.

The Canadian Hydrographic Service (CHS) has maintained a sea level gauge at North Sydney since 1970 (Fig 1A).

DATA AND METHODS

The sea level record shown in Honda and Dawson (1911) was digitized at 30-minute intervals then filtered (high-pass Butterworth filter, 4-hour cutoff) to focus on the high frequency seiche oscillations.

North Sydney sea level data were obtained from the Marine Environmental Data Service, Fisheries and Oceans Canada (MEDS, Ottawa, Canada <http://www.isdm-gdsi.gc.ca/isdm-gdsi/index-end.html>). The observations from 1989 to 1999 had a nominal sampling interval of 15 minutes which allows for the resolution of the high frequency seiches and longer period motions. During the period 1989-1999, the ~337,000 observations represent an 87.3% data return. Honda and Dawson (1917) and Easton (1994) reported only observing the fundamental seiche mode, with a period of ~2 h; this mode would be well-resolved in records with 15 minute sampling. The 15 minute sampling also can resolve the shorter period seiches indicated by Easton (1972).

Current meter and hydrographic observations were extracted from the Bedford Institute of Oceanography database (<https://www.bio.gc.ca/science/data-donnees/base/index-en.php>). The current meter data from the studies of Lane (1989) and ASA (1994) in the South Arm (Fig 1A) are particularly useful because their sampling interval of 15 minutes allows for the resolution of flows with periods longer than 30 minutes. The 2 single point current meter records from Lane (1989) were from just outside (13 m, bottom depth 14 m; 24 August-13 October 1987) and just inside the South Arm (14.6 m, bottom depth 16 m; 12 January-27 April 1988). ASA (1994) reports data for a single point current meter (10 m, bottom depth 16 m; 6 August-2 September 1992) and an ADCP (bottom-mounted, depth 15 m; 25 July-24 August 1993). These records are confined mostly to late summer-early fall, so an annual cycle of currents cannot be established. In October 2000, Fisheries and Oceans Canada (DFO) placed 2 ADCPs in the South Arm one (46.1521 °N, 60.2087 °W, bottom depth 14 m) just off the northern side of the mouth of Muggah Creek, the second (46.1503 °N, 60.2152 °W, bottom depth 12 m) 544 m to the WSW, off the western side of the Arm. Both moorings were recovered in May 2001, providing 216 days of observations sampled hourly. These records have not been reported elsewhere.

Amplitudes and phases were estimated from the datasets using harmonic analysis. Typically, the expression $A_0 + A_1 \cos(\omega(t-\phi))$ was used in a least-squares fit where A_0 is a constant (average value), A_1 is the amplitude of the harmonic which has a frequency $\omega (=2\pi/\text{period})$, t is time and ϕ is the phase. Both Butterworth high pass (cutoff at 4 h) and Loess filters were used to examine the low or high frequency components of the datasets. Power spectra (distribution of data variance with frequency) were estimated using the routine `pwelch` in Matlab.

RESULTS

Overall sea level and current variance

The overall variances of the sea level and current meter records are the result of many forcing mechanisms, including the flows driven by freshwater inflow (periods of days to annual cycles), long period tides and circulation changes outside the Harbour (solar annual

tidal constituent, annual water mass variations in Sydney Bight), meteorological forcing (wind stress, atmospheric pressure; periods of days to a year), tides (for Sydney Harbour the semi-diurnal {~twice per day} and diurnal {~once per day} tides are the most energetic), and the higher frequency seiches as noted by Honda and Dawson (1917) and Easton (1972).

The annual cycle of sea level variance by month was determined from the 1989-1999, 15-minute time series. Monthly values of variance were calculated for each year and then averaged across all years. It includes variability for periods ≥ 30 minutes and is a comprehensive estimate of the annual cycle of variance. The estimates, which lie between $\sim 0.092 \text{ m}^2$ (May-September; equivalent to an amplitude of 0.43 m) and 0.114 m^2 (January; 0.48 m), show a distinct annual variation, high during winter, low from late spring to early fall (Fig 2A). The greater part of the variance is due to the daily and twice daily tidal components. In fact, the variance of the five leading tidal constituents, M2, S2, N2, K1 and O1, alone is 0.083 m^2 , or 90% of the base variance of 0.092 m^2 . However, their contribution to the overall variance would be nearly constant every month, i.e., they would not contribute to the month-to-month variation (\equiv excess variance) seen in Fig 2A. Harmonic analysis shows that the excess variance is dominated by an annual cycle with an amplitude of 0.011 m^2 and a phase of 0.73 months (peak \sim Jan 23); it accounts for 88% of the variation. Potential sources of energy are wind-driven currents and their associated surface displacements; storms tend to be more numerous and stronger in winter than during summer. In addition, atmospheric pressure, generally lower during winter than in summer, could contribute. Based on the latest 30-y barometric pressure climatology for Sydney, the variance of this component is only 0.00015 m^2 , and therefore relatively insignificant. At higher frequencies, seiches generated by the wind could also contribute.

Low-frequency contributions to variance

A potential contributor to the annual cycle of sea level variance is the long period tides, notably the solar annual component (SA, period 365.24 days). In fact, the CHS reports a relatively large solar annual tidal constituent of 0.07 m with a peak amplitude in early December for North Sydney based on a 1-year record. However, if this were a pure tidal harmonic, its contribution to

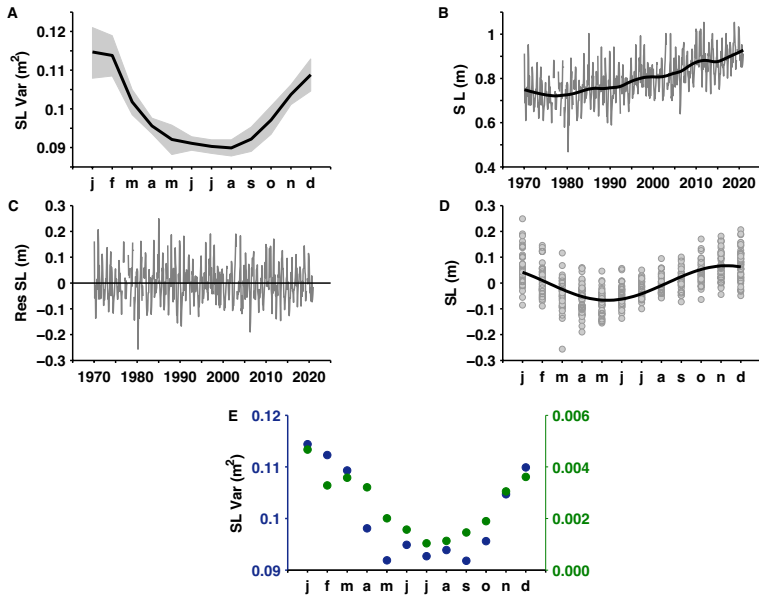


Fig 2 A) Annual cycle of sea level variance (SL Var, black line) and 95% confidence limits (grey shading) for Sydney Harbour based on North Sydney observations (1989-1999; 15 minute sampling). B) Monthly sea levels (SL, grey line) and long-term mean sea level variation (linear Loess 0.1 filter of monthly values, black line) 1970-2020 at North Sydney. C) Monthly sea levels with long-term variation removed. D) Annual harmonic of sea level (black line) based on the monthly observed values (grey points, 1970-2020; Fig 2C). E) Annual cycle of sea level variance (blue points) calculated from record sampled at 15-minute intervals; annual cycle of sea level variance from the monthly sampled record (green points).

the monthly variance would have a frequency 2 times the annual; its largest impact would occur at 3 and 9 months after the solar annual peak when the rate of change of the elevation associated with the annual harmonic is greatest; thus, it would be out of phase with the annual cycle of variance. Moreover, with an amplitude of 0.07 m, the largest contribution is only about 5% of the excess variance. Other factors such as changes in the water temperature and salinity and hence density, and annual variation of the current exterior to the Harbour can affect the annual cycle of sea level and emerge as a solar annual component in a short term (~1 year) tidal analysis. Annual cycles of temperature, salinity and circulation have been observed (Petrie and Drinkwater 1993, Drinkwater *et al.* 1979). This component of sea level can be examined by calculating

the monthly averaged sea levels (Fig 2B). The monthly averages effectively filter out the high frequency contributions to sea level including the dominant diurnal and semidiurnal tides, seiches and other short period variability.

The inter-annual variations of the annual cycle of monthly sea level are readily apparent along with a trend of increasing sea level (Fig 2B). Removing the trend (linear Loess 0.1 filter) shows the month-to-month variability more clearly (Fig 2C). Grouping the values by month reveals a distinct annual cycle (Fig 2D). Harmonic analysis gives an annual cycle with an amplitude of 0.067 m and a peak in early December, about 4 days later than the CHS result. The agreement is surprisingly good given the CHS result was based on a 362 day hourly record, whereas this analysis is based on a 5-decade series of monthly values. Note the greater scatter, i.e. increased variance, about the annual harmonic during the late fall-winter months than during the summer. The monthly variances (Fig 2D) are compared to the excess variance in Fig 2E. Although the patterns of both series – high in winter, low in summer – match well, the inter-annual variability of the annual cycle only accounts for about 13% of the excess variance. Steps to assess the contribution of inter-annual variability of the annual cycle are summarized in the Appendix.

The trend of increasing relative sea level at North Sydney is 39.1 cm/century (Hebert *et al.* 2021, see Fig 2B); where relative sea level refers to water level relative to a fixed benchmark on land). This is similar to trends of 37.5 cm/century for Yarmouth and 33.3 cm/century for Halifax. When corrected for post-glacial rebound (the crustal response to the retreat of the ice sheet; for all 3 sites, the crust is sinking), the trends are 27.2, 18.6 and 22.3 cm/century for Yarmouth, Halifax and North Sydney, respectively (Hebert *et al.* 2021). However, the trend for Halifax was based on the 1920-2020 data series, about 50 years longer than those for Yarmouth (1967-2020) and North Sydney (1970-2020). Using the 1970-2020 Halifax record, the relative sea level trend is 32.7 cm/century, 0.6 cm/century lower than the 1920-2020 trend. Hebert *et al.* (2021) do not offer an explanation for the different trends among the 3 sites.

Variance during summer versus winter

The contributions to the variance over a broad range of frequencies can be investigated by comparing the winter and summer sea

level spectra. For 1989-1999, spectra could be computed for records of January-February-March (winter) sea level for 1990, 1991, 1993 and 1995, and for July-August-September (summer) for 1991-1994 and 1999. The average winter spectrum is generally greater across all frequencies than the average summer spectrum (Figs 3A,B). Several features emerge: the greatest increases of variance occur at frequencies of 0.2 to 1 cpd (cycles per day; Fig 3B).

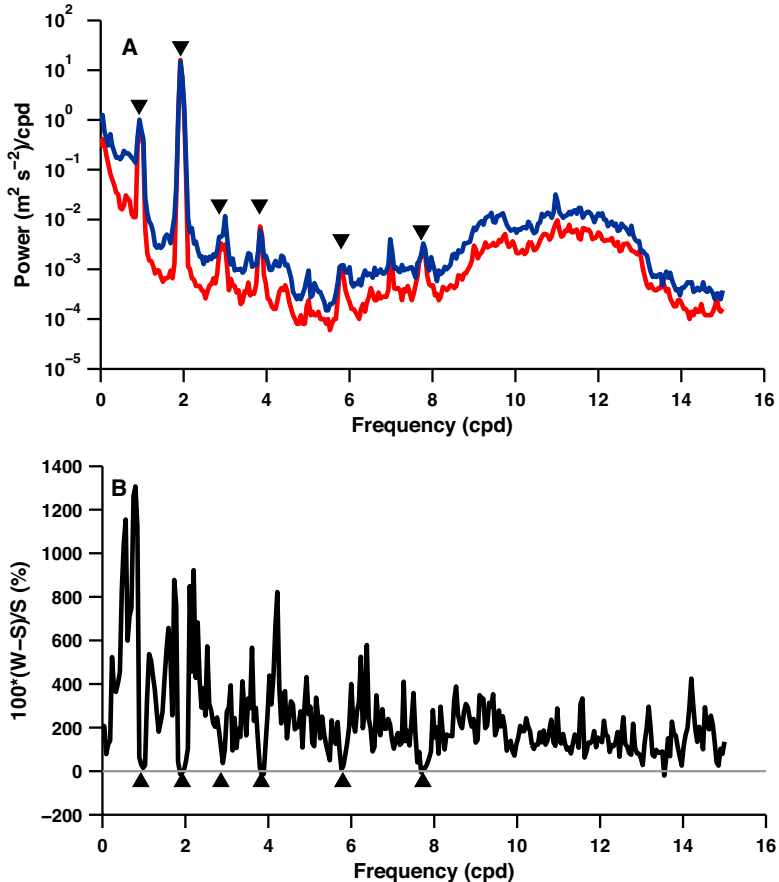


Fig 3 A) Average sea level winter (summer) spectrum (January-February-March, blue; July-August-September, red) derived from 15 minute observations at North Sydney. Spectra cover frequencies from 0.047 to 48 cpd; frequencies higher than 15 cpd had little energy and are not shown. B) Percentage difference of winter spectrum relative to the summer spectrum. In both panels, triangles indicate frequencies of tidal constituents at approximately 1, 2, 3, 4, 6 and 8 cpd.

Integration over this band yields an equivalent amplitude of 0.058 m for summer and 0.144 m for winter. These values differ significantly at the 95% confidence level. The largest contributions by far to the overall variance are from the semi-diurnal and diurnal tides; on the other hand, the summer-to-winter differences at tidal frequencies, approximately 1, 2, 3, 4, 6 and 8 cpd (cycles per day; periods of 24, 12, 8, 6, 4 and 3 h), are close to 0, which is expected (Fig 2B). The appearance of tidal harmonics, constituents caused by non-linear effects, near 3, 4, 6 and 8 cpd, is novel given the low tidal velocities. Integrating across the spectral peaks near these frequencies gives amplitudes of 13, 0.8, 0.5 and 0.8 mm; this compares favourably with the CHS tidal constituents of 3.5 mm average value of 7 constituents at ~ 3 cpd, 4 mm for 4 constituents at ~ 4 cpd, 2.2 mm for 2 at ~ 6 cpd, and 2.6 for 4 constituents at 8 cpd (analysis from P. MacAulay, CHS, Bedford Institute of Oceanography).

In summary, the increased sea level variance during the winter compared to summer appears due to a general rise across all frequencies with the exception of the tides. Greater increases of variance are found in the storm band (frequencies 0.2-1 cpd). The winter to summer difference in variance ($0.0193 \text{ m}^2 \text{ s}^{-2}$, Fig 2A) matches the difference ($0.0188 \text{ m}^2 \text{ s}^{-2}$) calculated by combining the integrals over the spectra (Fig 3A) and the variance due to the annual cycle (Fig 2E).

Seiches

Honda and Dawson (1911) show only 21 hours of observations of the month-long sea level record of 1901 at Battery Point. A digitized, high-pass filtered time series of their Plate 1 (Fig 4A) shows seiche amplitudes as large as ~ 0.2 m with an average period of ~ 125 minutes, agreeing well with their estimated period of 132 minutes for the South Arm (note that the average depth stated by Honda and Dawson (1911) for the Harbour was 4.1 m, likely an error as the average depth is ~ 10 m; moreover, using their stated depth, the fundamental periods would be 179 and 197 minutes, considerably longer than the 120 and 132 minutes they reported).

Easton (1972) calculated resonant periods of 103, 52, 36.6 and 22.5 minutes for the first four modes of his three-channel model of the Harbour. The depth and width of each channel was constant but differed among the three. He refined this idealized model by incorporating variations in depth and cross-section; he solved the finite difference forms of the governing equations, obtaining resonant periods

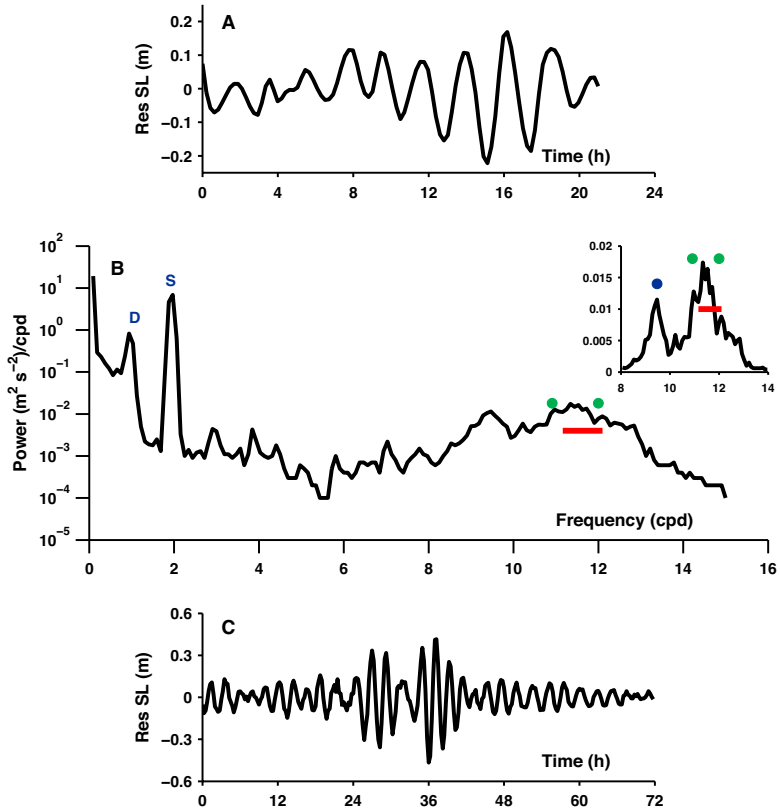


Fig 4 A) High-passed (cutoff at 6 cpd) sea level record from Honda and Dawson (1911). From hour 8 to 20.5 there are ~ 6 cycles which gives an average frequency of 11.5 cpd. B) Spectrum of North Sydney sea level observations (January 27-June 27, 1990; 15-minute sampling interval). The dominant diurnal (D) and semi-diurnal (S) peaks are evident; in addition, a broad spectral peak encompassing the seiche fundamental mode is indicated (green dots are the 2 fundamental periods calculated by Honda and Dawson (1911), the red line represents the seiche frequency band predicted by Easton (1972)). The inset magnifies the structure in the seiche band and shows an estimated, typical edge wave frequency (blue dot) predicted by Easton (1972). C) Highest sea level seiche amplitude burst for the period January 27-June 27, 1990 occurred from February 24-27, where hour 0 corresponds to 00:00 February 24.

of 107, 39, 31.5 and 24 minutes at mean water level, different from the periods based on the 3-channel model. Repeating the calculations for high and low tidal elevations modulated the period of the first mode by a range of 10 minutes. Further, a correction for the Harbour opening onto the ocean increased its period from 107 to 124 minutes.

Easton presented only 12 h of the 1970 sea level records from North Sydney he analyzed; his Fig 1 shows a distinct seiche with a peak amplitude of ~ 0.28 m and a period of ~ 123 minutes. He reported distinct oscillations with periods in a narrow band of 120 to 130 minutes lasting for 12 hours to 3 days and amplitudes as large as 0.6 m. This corresponds to an average current at the mouth of the Harbour of ~ 0.25 m s⁻¹ ($= 2 \times 0.6 \text{ m} \times 54.4 \times 10^6 \text{ m}^2 / (73 \times 10^3 \text{ m}^2 \times 3600 \text{ s})$, where 54.4×10^6 is the surface area of the Harbour, 73×10^3 is the cross-sectional area at the mouth of the Harbour). Easton (1972) concluded that the seiches were initiated by storms and were probably the response to external edge waves, whose periods he estimated as about 152 minutes. External edge waves, generated by passing atmospheric disturbances, are natural, oscillatory motions over a sloping bottom at the coast. Their crests are normal to the shoreline and travel in a direction parallel to the shore. Wave amplitudes diminish rapidly with offshore distance (within ~ 10 km).

The amplitude structure of the fundamental seiche mode from Easton's model indicates that the highest sea level elevations are found at Sydney River, the head of the South Arm. Relative to a peak magnitude of 1 at the head of the South Arm, the amplitude decreases to 0.93 at Battery Point where Dawson's observations were taken, and to 0.79 at the mouth of the Arm. At the site of the CHS gauge at North Sydney, the amplitude further decreases to 0.74. This suggests that the seiche amplitudes in the South Arm might be as much as 35% higher at its head and 26% higher at Battery Point than those recorded by the CHS gauge.

To examine further the predictions of Honda and Dawson (1911) and Easton (1972), sea level data were obtained from MEDS. Data are available at sampling intervals of 1 and 15-minutes, 1-hour, and 1-day depending on the year. However, only hourly and daily formats, sampling frequencies inadequate to resolve the seiche periods, were available for the 1970 data examined by Easton (1972). Instead, a 5-month long series sampled at 15-minute intervals from 1990, the earliest that could adequately resolve the seiche activity in the Harbour, was analyzed.

Fig 4B shows the power spectrum (the distribution of variance per unit frequency versus frequency) of the North Sydney sea level record which runs from January 27 to June 27, 1990. The spectrum shows the expected tidal peaks around ~ 1 cpd (diurnal) and

~2 cpd (semi-diurnal) as well as a broad peak, centred at ~12 cpd, the expected periods of the two fundamental modes of the Harbour estimated by Honda and Dawson (1911). Integrating the spectrum across this frequency band (inset, Fig 4B) yields an average harmonic amplitude of 0.066 m. This indicates that seiches can make significant contributions to sea level variability in the Harbour, compared to the leading diurnal component (K1, 0.93 cpd) with an amplitude of 0.082 m and the largest semi-diurnal component (M2, 1.93 cpd) at 0.38 m. There are 2 peaks evident in the 8-14 cpd band: the first at (~11.4 cpd (period 126 minutes, inset Fig 4B) corresponds to the fundamental seiche periods of Honda and Dawson (1911) and Easton (1972); the width of this peak (~1 cpd) is the same as estimated by Easton (1972) as the variation of the seiche period due to high and low water levels due to tidal variations. The second peak, at 9.47 cpd (152 minutes), corresponds to the edge waves suggested by Easton (1972) as the external driver of the seiches in the Harbour. During this 6-month period, a peak seiche amplitude of ~0.45 m occurred in late February (Fig 4C).

The Easton (1972) model indicates that the seiche amplitude averaged over the South Arm should be 1.24 times larger than at the North Sydney tide gauge. For the following estimates though, it is assumed that the elevations observed at North Sydney apply to the South Arm. The average current across the mouth of the South Arm required to give the observed sea level elevations (from minimum to maximum elevation) associated with the tides and the seiche band can be estimated as $4A_s\zeta/(A_x\tau)$, where A_s is the surface area (=11.1 km²) of the South Arm, ζ is the sea level amplitude, A_x is the cross-sectional area (27265 m²) of the mouth of the Arm, and τ is the period of the component in question. For a seiche with a sea level amplitude of 0.066 m, the current would be 0.015 m s⁻¹. Easton (1972) indicates that seiche amplitudes of 0.15 m are common; this would correspond to currents of 0.035 m s⁻¹. The peak amplitude of 0.6 m he reported corresponds to a 0.15 m s⁻¹ flow. Ninety-five percent of the 1989-1999 15-minute observations in the high-pass series were less than 0.141 m; about 1% of the observations exceeded 0.2 m.

Forces driving the seiches

The response of Sydney Harbour can be examined in light of the classic, externally-forced single-degree-of-freedom model of a rectangular harbour developed by Miles and Munk (1961, Fig 5A).

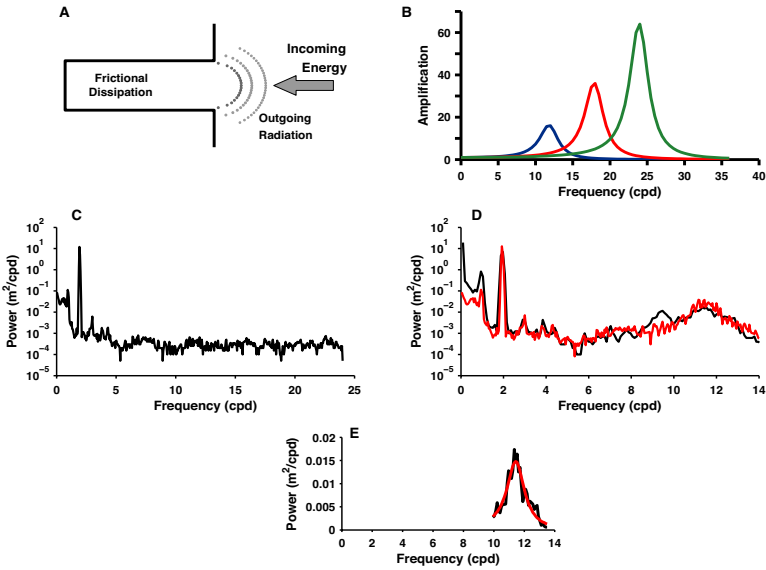


Fig 5 A) Schematic of Miles-Munk (1961) harbour model. The large grey arrow depicts the incoming energy from the adjacent ocean. Frictional dissipation within the harbour is due to current flow over the harbour bottom. The dots outside the mouth of the harbour illustrate energy radiated back to the ocean. B) Amplification factor for resonant periods of 12 (blue) 18 (red) and 24 (green) cpd with Q values of 4, 6, and 8 respectively. C) St. Ann's Bank winter-spring sea level spectrum which serves as the input of the model. D) Comparison of North Sydney sea level spectrum (black, see Fig 4A) with model spectrum (red, =St. Ann's Bank spectrum * model response function). E) Smoothed, least-squares best fit of model response function to North Sydney sea level spectrum (see Fig 4B) in frequency band of 10-13.5 cpd.

While the passage of an atmospheric pressure front or wind shifts can generate seiches directly within the harbour, Miles and Munk (1961) maintained that excitation through the harbour mouth by the broad spectrum of external wave-like motions is the main cause. The sea level response of the harbour depends its natural frequency, which in turn rests on the harbour's geometry, the frequency of the incoming energy, dissipation within the harbour and the radiation of energy from the harbour mouth back out to sea. They parameterize the overall dampening of the seiche as inversely dependent on the parameter Q which is composed of two parts, frictional dissipation in the harbour and radiation of energy back into the open ocean. A harbour with a low (high) value of Q both adjusts to the incoming external wave motions and dampens the harbour response quickly (slowly).

Fig 5B illustrates the impact of Q on harbour response with lower power amplification with $Q = 4$ (more dampening), resonance period energy magnified by a factor of 16, and greater amplification with $Q = 8$ (less dampening), magnification by a factor of 64. Miles and Munk (1961) argue that the main dampening mechanism generally is the radiative loss of energy through the harbour mouth rather than through bottom friction within the harbour.

By combining an offshore sea level spectrum with the Miles-Munk model, the harbour response can be estimated and compared to the observed response within the harbour. The offshore spectrum comes from a bottom pressure gauge on a mooring located on St. Ann's Bank (46.18 °N, 60.22 °W) about 83 km east of Sydney Harbour, water depth 108 m (Fig 5C). The data were collected during the winter and spring of 2015 and therefore are not contemporaneous with the North Sydney sea level observations. Nonetheless, they should provide some insight on how the offshore energy is amplified in the harbour. Between 5 and 24 cpd, the spectrum is quite flat with an integrated amplitude equivalent to 0.107 m sea level displacement. This spectrum serves as the input to the Miles-Munk model and the resulting response for the harbour (red line, Fig 5D) is compared to the observed response (black line, Fig 5D). Focussing on frequencies near the expected fundamental resonance (10-13 cpd), the agreement of the modelled (St. Ann's spectrum* model amplification) and the observed North Sydney sea level spectra is excellent. On the other hand, at frequencies of ~ 9 cpd, the observed spectrum is consistently more energetic than the modelled one. However, this is precisely (at 9.5 cpd) where Easton (1972) expected to find coastally-trapped waves whose amplitude are likely attenuated at the offshore St. Ann's Bank mooring site. Munk *et al.* (1956) give the offshore scale, L , of the edge waves as $U^2/g \cdot \sin(\beta)$, where U is the speed of the travelling disturbance and β is the bottom slope. Using the values in Easton (1972) gives an offshore scale of ~ 10 km. It is reasonable then that the energetic edge waves at ~ 9.5 cpd are attenuated at St. Ann's Bank and therefore not present in the record. The amplification function used in the spectral comparison (Fig 5D) was based on a least-squares fit in the frequency band 10-13.5 cpd (Fig 5E). The fit ($R^2 = 0.89$) gives a Q of 8.3 at a resonant frequency of 11.5 cpd (period of 125 minutes); Easton's (1972) model found a resonant period of 124 minutes.

Currents associated with seiche oscillations

A 100 h segment (Oct 2-6, 1987) of the recorded, along-harbour currents (blue line, Fig 6A; data from Lane (1989, 1991)) from just outside of the mouth of the South Arm of Sydney Harbour shows the dominant flows, the underlying semi-diurnal tidal current (shown in red for clarity) and the high frequency seiche motion with a period of ~2 h (Fig 6B).

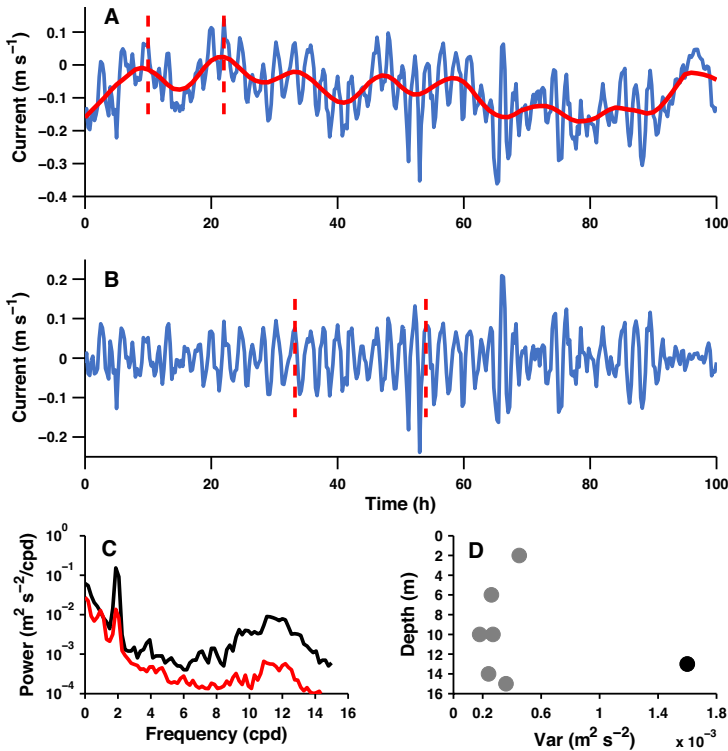


Fig 6 A) Section (Oct 2-6, 1987, blue line) of the current meter record from just outside the mouth of the South Arm of Sydney Harbour; data shown are positive along 178°, the direction of maximum variance and approximate orientation of the South Arm. The red line is a filtered version to emphasize the tidal flows. Vertical red lines span 12 hours. B) Time series of current meter record shown in Fig 6A after it has been processed using a high pass filter. The vertical red lines correspond to a time span of 20.75 hours. C) Spectra of the current meter time series from outside the mouth of the South Arm resolved along 178° (black line), and from the ASA ADCP series in the South Arm (red line), the average of the 2, 6, 10 and 14 m spectra. D) High frequency variance of current meter data from the moorings in the South Arm (grey points) and just outside the mouth of the South Arm (black point; see Fig 1A, B for locations). Five of the six records from the South Arm are from August, one from Jan-Apr.

The seiche current has a representative speed of $\sim 0.07 \text{ m s}^{-1}$ and a peak flow of 0.24 m s^{-1} , stronger than the tidal current amplitude of $\sim 0.04 \text{ m s}^{-1}$.

The power spectra of series outside and inside the South Arm show the expected strong semi-diurnal peak at ~ 2 cpd and the broad peak centered about 12 cpd (Fig 6C). The outer spectrum is more energetic than the one from within the Arm. The ratio (outside/inside) of the variances for the band 10-14 cpd is ~ 13 . The semi-diurnal tidal band corresponds to an amplitude of 0.114 m s^{-1} , the seiche band to 0.049 m s^{-1} for the outer series, whereas, for the South Arm record, the equivalent currents are 0.019 and 0.01 m s^{-1} .

The high frequency variance outside the mouth is about 5.5 times greater than that within the Arm (Fig 6D). However, it should be noted that these records are not contemporaneous.

The current meter data consist of short records and for the greater part are confined to the summer months (5 of 6 are from August, 1 from January-April) when seiche activity might be reduced. We can use the sea level data subjected to a high pass filter and continuity (flow into (out of) the harbour gives rise to an increase (decrease) of sea level) to obtain some idea of currents in the South Arm. Seiche current estimates were made using the high pass filtered 1989-1999, 15-minute sea level observations from the North Sydney gauge; their distribution suggests that most current speeds are low, 79% are less than 0.02 m s^{-1} . These estimates are in excellent agreement (root mean square difference = 0.34%) with the combined current meter data observations in Table 1.

Table 1 Comparison of the percentage distributions of seiche current speeds estimated from sea level observations (SL, 336,577 points) and in situ current meter data (CM, 23,208 points). Maximum in situ current speed was 0.24 m s^{-1} .

m s^{-1}	0-0.02	0.02-0.04	0.04-0.06	0.06-0.08	0.08-0.10
SL	78.8	17.9	2.6	0.41	0.092
CM	78.0	18.4	2.4	0.074	0.211

Table 1 cont'd

m s^{-1}	0.10-0.12	0.12-0.14	0.14-0.16	0.16-0.18	0.18-0.20	>0.20
SL	0.028	0.010	0.0032	0.0021	0.0015	0.0006
CM	0.069	0.047	0.0043	0.0043	0.0043	0.013

Tidal flows

The ASA (1994) study tabulated the results of analyses of the tidal currents in Sydney Harbour, including ADCP records from off Muggah Creek sampling from 2-14 m at 1 m resolution (Fig 1A for location). Using those tables, we find that the amplitude along the major axis of the tidal ellipse of the principal semi-diurnal constituent, M2, was ~23 times greater (median value of the 13 depths) than along the minor axis; the major axis was oriented along the harbour at all depths (range of direction was from 155° to 162° True). In Table 2, the currents at the mouth of the South Arm derived from harmonic analyses of sea level amplitudes from the North Sydney gauge are compared to results presented in the ASA (1994) report for the single point current meter and the ADCP. The sea level-derived currents for the 5 principal tidal components are given by the formula $U = 2\pi * A_s * \zeta / (A_x * \tau)$. The current phase should lead the sea level phase by 90°. The tidal flows are quite small with only M2 currents exceeding 0.01 m s⁻¹; moreover, 8 of 9 comparisons are within 0.005 m s⁻¹ of each other, the exception is the M2 current for 1993. The comparison illustrates the utility of simple principles, in this case continuity, given the availability of long-term observations of sea level to estimate current velocities.

Table 2 Comparison of the tidal flows along axis of Sydney Harbour derived from sea level elevations (U) and from ASA moored current meters, at 10 m in 1992 and 1993.

	M2	S2	N2	K1	O1
Period (h)	12.42	12	12.66	23.93	25.82
Z (m)	0.368	0.109	0.076	0.077	0.082
U (m s-1)	0.021	0.006	0.004	0.002	0.002
ASA 1992 (m s-1)	0.017	0.006	-	0.007	0.003
ASA 1993 (m s-1)	0.008	0.005	0.004	0.002	0.003

To complete the picture, the depth profiles of the M2 (principal semi-diurnal) and K1 (principal diurnal) major axes current amplitudes and phases are shown in Fig 7. While there is a systematic variation of amplitudes and phases with depth, with such low velocities a detailed investigation is not pursued here. However, given the relatively short (~1 month) duration of the record during the summer when stratification is strong, an M2 internal tide, with opposing velocities in the upper and lower layers superimposed

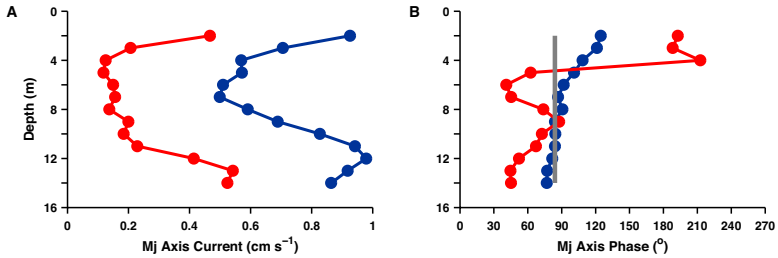


Fig 7 A) Depth profile of M2 (blue) and K1 (red) major axis currents in the South Arm of Sydney Harbour. B) Depth profile of M2 (blue) and K1 (red) major axis phases. Tidal analyses are based on a 1993 ADCP record collected by ASA (1994). Grey line represents the M2 current phase calculated from the M2 tidal constant derived from the North Sydney sea level record.

on the usual tide (i.e. velocity constant with depth), could cause the observed velocity and phase structure. Note the M2 current phase, a measure of the temporal relationship of this component to the lunar forcing, derived from the sea level data agrees with the phases calculated from the in situ ADCP observations (Fig 7B). At the latitude of Sydney Harbour, diurnal internal waves cannot be generated, though other types of waves with vertical structure can exist and lead to variations of velocity and phase with depth. The weak tidal currents suggest they play only a minor role in the dynamics of the South Arm of the Harbour. In fact, using representative velocities for the Harbour to examine the M2 dynamics, the acceleration terms exceed the frictional terms by a factor of 50. By comparison, the peak seiche velocities, while episodic, can exceed 0.1 m s^{-1} , an order of magnitude greater than that of the tidal components.

Mean flows

The South Arm features surface outflow and mid-depth and deep inflows (Fig 1B) and given the freshwater inflow from Sydney River, this is consistent with estuarine circulation (e.g., Geyer and MacCready, 2014). The mean currents along and across the Arm from the DFO deployment suggest the same picture: near-surface currents are northward, towards the mouth, deeper flows are towards the head (Fig 8A,B). It is apparent that these profiles have more inflow than outflow. To achieve a local balance requires a surface current of $\sim 2.5 \text{ cm s}^{-1}$ at the western mooring which seems reasonable; on the other hand, a surface flow of 7.9 cm s^{-1} would be

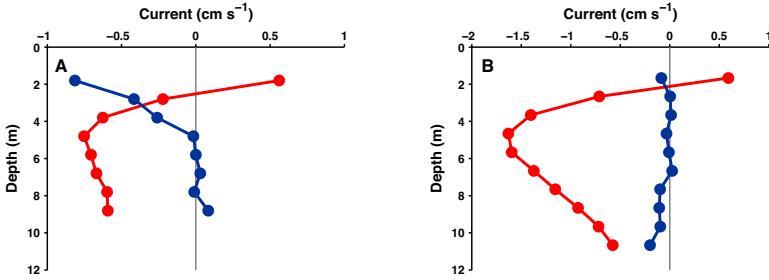


Fig 8 A) Profile of mean along-harbour (positive towards 10° True, red) and across-harbour (positive towards 100° True, blue) currents from the DFO deployment off the western side of the South Arm May 2001-Oct 2002. B) Profile of mean along-harbour (positive towards 2° True, red) and across-harbour (positive towards 92° True, blue) currents off Muggah Creek May 2001-Oct 2002.

necessary for the mooring off Muggah Creek. This flow is much stronger than any of the observed mean currents and seems more unlikely. Combining the 1 m vertical resolution of the moorings and representative widths across the Arm for the 2 moorings at each depth, there is a net transport towards the head of $\sim 63 \text{ m}^3 \text{ s}^{-1}$. To balance this flow requires an outflow of 0.047 m s^{-1} in the surface layer ($\sim 1.2 \text{ m}$ not sampled by the instruments) across the breadth of the Arm. Though high relative to all the measurements, a current of this magnitude cannot be ruled out. On the other hand, these two moorings, despite their proximity, may not have sampled the spatial structure of currents adequately.

Hydrographic sections along the axis of the South Arm in May 2001 and October 1999 reinforce the estuarine nature of the circulation. The temperature and salinity sections from May 2001, a period when stratification is developing, are characterized by 3 layers (Fig 9A,B): the first, from the surface to $\sim 2 \text{ m}$, is highly variable along the Arm. Within 2 km of Sydney River, the salinity increases rapidly from about 4 to >27 , suggesting strong entrainment of deeper, saltier waters into the river discharge. Areas of relatively warm, freshwater are interrupted by stretches of cooler, saltier water. The transit time in the surface layer from the head to the mouth $\sim 10 \text{ d}$ (13 km at a representative velocity of 0.01 m s^{-1}) coupled with varying freshwater inflow could have contributed to the variation of salinity. From 2 to 9 m, the structure is more uniform with temperatures of 2-3 °C and salinities of 27-28. Below 9 m, temperatures are 0-1 °C, salinities generally >29 . The October sections feature

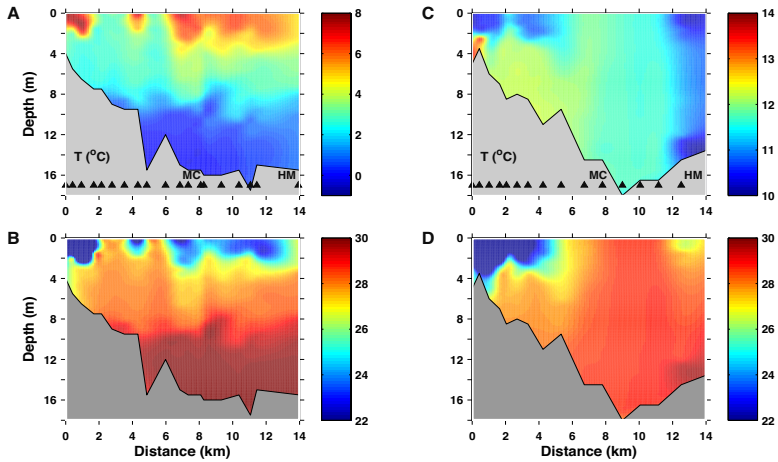


Fig 9 A) Temperature section along the axis of the South Arm, May 2001, from just seaward of Sydney River (distance 0 km) to outside the mouth. Temperature/salinity stations are indicated by an arrowhead at 17 m. The locations of Muggah Creek (MC) and the Arm mouth (HM) are shown. B) Salinity section. C) Temperature and D. salinity sections, Oct 1999.

weaker vertical gradients than in May, with the exception of the pronounced wedge defined by salinity beginning at Sydney River and extending nearly 5 km down the Arm (Fig 9C,D). The surface salinity was ~ 4 , the 4 m salinity was 25.6 at the first station in this section; 5 km along the Arm, surface salinity was 26.4. The wedge was a region of strong entrainment from the deeper waters into the surface layer. Vertical gradients of temperature and salinity in the outer half of the Arm are weak likely due to a breakdown of stratification at this time of the year.

DISCUSSION

More than a century ago, Dawson began the collection of sea level observations for Sydney Harbour as part of broader program focused on safe navigation in ports and in open water shipping lanes on the Canadian Atlantic coast. In 1970, the Canadian Hydrographic Service continued this work through the establishment of a tide gauge at North Sydney, maintained to this day and the basis for much of the analysis presented here.

There is a distinct annual cycle in sea level variance – high during the winter, low from late spring to early fall – that is the result

of increased energy across all frequency bands with the exception of the tides. The largest increases were in the storm band (0.2-1 cpd).

Dawson observed a high frequency seiche in the South Arm of Sydney Harbour with a dominant period of ~ 2 h and elevations comparable to those of the tidal constituents. In collaboration with Honda, the seiche was identified as the fundamental harbour mode. The spectrum of the record presented here featured a seiche with a period of 125 minutes, essentially the same as that derived by Honda and Dawson (1911) and Easton (1972). In addition, another spectral peak was identified at 152 minutes, the same period calculated by Easton (1972) for external edge waves hypothesized to drive seiches in the Harbour.

Given the importance of seiches in the Harbour, an analysis of frequency of occurrence of sea level elevations was conducted. The results (based on the 1989-1990, 15-minute, $\sim 336,000$ observations, filtered to retain frequencies > 6 cpd) indicate that 50% exceeded 0.05 m, 5% were greater than 0.136 m, 0.01% exceeded the M2 tidal amplitude of 0.38 m. The maximum observed amplitude was 0.74 m. The maximum seiche current was 0.24 m s^{-1} from the limited in situ current meter data. Easton's (1972) model suggests that the seiche amplitudes in the South Arm might be as much as 35% higher than those recorded by the North Sydney gauge. However, a comparison of a limited series of surface elevations in the South Arm with contemporaneous North Sydney data suggests the amplification indicated by Easton (1972) was overestimated (Fig A2).

The analysis of current meter data (Fig 7C) indicates substantially more energy in the seiche band outside the South Arm with the ratio (outside/inside) of variances about 13. Easton (1972) gives the structure of the current transports along the Harbour for the first modes. To convert transport to current requires knowing the cross-sectional areas used in the model, however, they are not given. Using the chart for Sydney Harbour to estimate the cross-sections yields a ratio of current variances of 4-12, the major uncertainty arising from the estimate of the cross-section outside the Arm at the current meter site. Given that the current series were collected at different times, the comparison lends some support to the model.

Application of the Miles-Munk (1961) spectral model suggested that offshore forcing does indeed drive a response in the Harbour with the dissipative parameter $Q = 8.3$. This compares with values

of 2.3 (more dissipation/radiation) for Oceanside, California and 11.2 (less dissipation/radiation) for Acapulco, Mexico which were estimated from the data in Miles and Munk (1961). From Okihiro *et al.* (1993), a Q of 8.8 was calculated for the fundamental mode of Barbers Point Harbor, Hawaii, which is about one tenth the size of Sydney Harbour. Okihiro *et al.* (1993) identified two other higher frequency but lower energy seiches in the sea level spectra from the Harbor. One appears to be the first harmonic of the fundamental mode; the second appears to be a separate harbour mode. Garrett (1972) calculated a Q of 5.3 (± 1.5) for the Bay of Fundy. He found that the radiative component ($Q_R = 6.8$) dominated the dissipative component ($Q_D = 18.2$), however, he argued that the estimate of Q_D “seems rather high”. In the end he states, “It seems unlikely that Q_D for the whole system could be more than about 10.”

Both Honda and Dawson (1911) and Easton (1972) mentioned only observing the fundamental mode for Sydney Harbour. The CHS and the Marine Environmental Data Service (Fisheries and Oceans Canada, Ottawa) provided sea level records from North Sydney sampled at 1-minute intervals which enabled the higher modes to be resolved. The spectrum of a record from Jan 4-May 26, 2015 shows the fundamental (zeroth, ~ 11.6 cpd) mode as the most energetic (Fig 10). Mode 1 (31.6 cpd from Easton’s (1972) model) does not

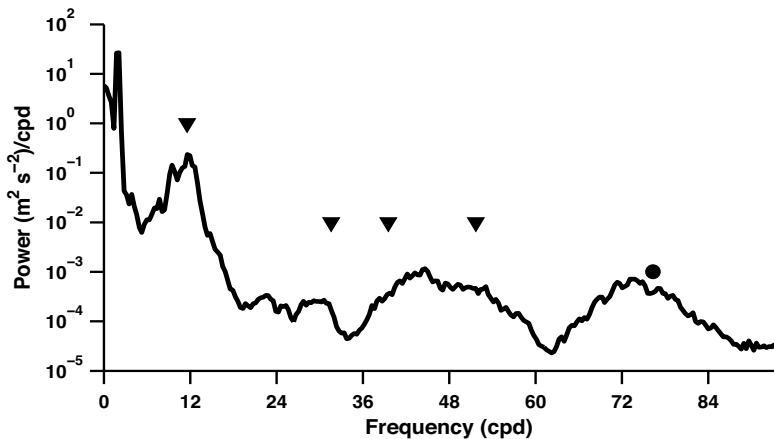


Fig 10 Spectrum of North Sydney sea level. Record was from Jan 4-May 26, 2015, sampled at 1-minute intervals. The downward arrows are the seiche frequencies (modes 0-3, where 0 is the fundamental mode) predicted by the model of Easton (1972). The dot is mode 4 projected from modes 1-3.

seem to be present, consistent with Easton's result that indicates a nodal point for this mode near the North Sydney tide gauge. Modes 2 (39.5 cpd) and 3 (51.7 cpd) correspond to a broad peak from 33 cpd to 62 cpd. The projected mode 4 at 76.3 cpd corresponds to a second broad peak from 62 cpd-88 cpd. In this spectrum, the fundamental mode is equivalent to an amplitude of 0.064 m (integration from 11-14 cpd), the broad peak for modes 2 and 3 to 0.01 m, and the projected mode 4 to 0.0075 m. Clearly, the fundamental mode dominates; the higher order modes reported here have variances 2.3% (modes 2, 3) and 1.4% (mode 4) of the fundamental.

Tidal currents in the South Arm are weak with the leading M2 constituent having an along-harbour velocity of 0.01 m s^{-1} . The appearance of tidal harmonics (e.g., Fig 3A), usually confined to areas, such as the Bay of Fundy, where tidal velocities are strong and frictional dissipation is large, was surprising. The mean flows also were weak with speeds of about 0.01 m s^{-1} .

Given the relatively strong freshwater inflow from Sydney River, it is reasonable to expect estuarine circulation dominating the mean flows in the Arm. The limited hydrographic data, showing strong gradients in the first 2 to 5 km from Sydney River, support strong entrainment of deeper saltier waters into the surface layer.

Despite the weak mean circulation in the South Arm, the distribution of polycyclic aromatic hydrocarbons (PAH) in the sediments suggests the average currents may play an important role. Vandermeulen (1986) indicated that the major source of PAH is from Muggah Creek. The map of PAH concentrations in the Harbour shows by far the largest concentrations at and just outside of Muggah Creek (Fig 11). The inset depicts the concentrations on the eastern side of the South Arm, with the tendency of higher values towards Sydney River rather than towards the mouth. Petrie *et al.* (2001) used the Lane January-April 1988 current meter data to drive a bottom boundary layer model to examine the re-suspension, transport and re-settling of sediments (bbbt; Hannah *et al.*, 1995). In the model, bottom sediments were characterized by a distribution of critical stress values – at low stresses only the finer fraction would resuspend; as currents and consequently stresses increased, a larger fraction of the sediments would be lifted into suspension. Once suspended, the sediments are subject to the vertical structure of the currents and vertical mixing. For the January-April period,

there were 17 events when at least 40% of the sediment was re-suspended. As the sediments sank and re-settled, their overall tendency was to move upstream towards Sydney River and re-settle on the bottom. These results are consistent with the measured bottom concentrations of PAH shown (Fig 11). More recently, analysis of cores for metals and organic contaminants in Sydney Harbour by Smith *et al.* (2009; see Table 3) show elevated levels of lead and PAH inventories towards the head of the Arm relative to those towards the mouth in agreement with the observations presented by Vandermeulen (1986).

While his main objectives were to acquire sea level data for ports and shipping lanes for Atlantic Canadian waters and to establish a long-term tide gauge network, nonetheless, W. Bell Dawson spent time exploring the dynamics of the time series he acquired. Consequently, he identified the seiches in Sydney Harbour and

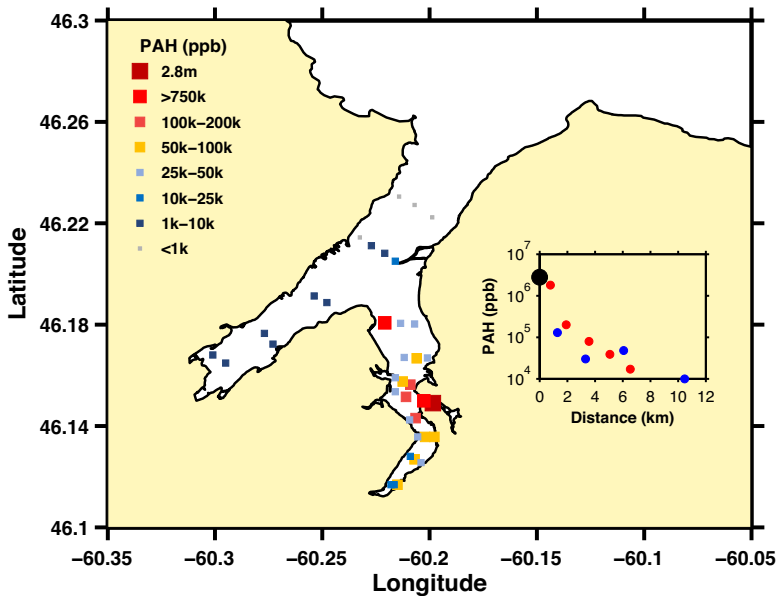


Fig 11 Map of PAH stations and concentration in parts per billion. Stations are colour- and size-coded according to concentration. The inset shows the PAH concentrations of stations on the eastern side of the South Arm. Red dots are for sites located in the South Arm on the Sydney River side of Muggah Creek, blue for sites towards the mouth of the Arm. Note the high concentration of PAH on the western side of the South Arm near the mouth. This was a dump site for material dredged in the South Arm. Data are from Vandermeulen (1986).

Table 3 Lead (Pb) and PAHs inventories of cores from the eastern side of the South Arm. Data from Smith et al. (2009), their Table 1. Negative (positive) distances are towards Sydney River (mouth of South Arm). Distances are from the mouth of Muggah Creek. Station 4b of Smith *et al.* (2009), just outside of Muggah Creek, is the reference station. Npts is number of cores.

Distance (km)	-3 to -2	-2 to -1	-1 to 0	Sta. 4b at 0	0 to 1	1 to 2	2 to 3
Pb ($\mu\text{g cm}^{-2}$)	1918	4195	3758	4507	2435	2621	2026
Npts	3	1	5	1	3	3	2
PAHs ($\mu\text{g cm}^{-2}$)	881	2268	6211	9905	2544	2023	
Npts	1	2	1	1	2	1	0

recognized their importance to navigation and to conducting port activities safely. His foresight in developing the sea level network and CHS's ongoing maintenance of a gauge at North Sydney enabled the analyses presented here, an extension of research that began more than a century ago.

CONCLUSIONS

Seiches in Sydney Harbour, given their episodic nature and high frequency, have elevations that can exceed the amplitude of the major tidal constituent M2 by a factor of 2; seiche currents in the Arm were ~ 10 times greater than tidal or mean flows. Consequently, their impact on harbour shipping and safety could be significant. The strong flows due to seiches have the potential to resuspend sediments and affect their distribution on the harbour bottom. Though weak, the persistence of the mean circulation can act to retain contaminants associated with sediments in the South Arm.

The circulation derived from moored instruments and the temperature and salinity sections suggest the development of basic circulation models based on mass and salt conservation, entrainment and two-way vertical exchange. Such models, e.g. for Halifax Harbour, have been successfully applied to hindcast nutrient, dissolved metals, suspended solids and bacterial transport and distribution within the harbour and to forecast changes due to modifications such as sewage treatment (Petrie and Yeats 1990). A proxy for freshwater inflow would be required, likely based on rainfall (or nearby gauged rivers) and drainage basin area since Sydney River has never been gauged.

Simultaneous measurement of sea level at North Sydney and in the South Arm with a sampling rate of at least 15 minutes could verify the Easton (1972) model more definitively than has been possible with the existing observations.

Acknowledgements I thank David Greenberg and Adam Drozdowski for their reviews which helped to clarify the text. Adam Drozdowski raised a number of issues that led to further analyses particularly with respect to potential drivers of the seiches, structure of Easton's (1972) modes and the net transport in the South Arm. My thanks to Phillip MacAulay (CHS) for suggesting the use of the 1-minute sea level data and Jenny Chiu (MEDS) for compiling the times series for 2015-2017. The analysis of these data showed the higher modes in the Harbour that it was not possible to investigate with the series sampled at 15-minute intervals. There were also several useful discussions with Phillip MacAulay on various aspects of seiche activity in coastal embayments. My thanks to the 2 external reviewers for their careful reading of the manuscript and positive suggestions to improve clarity and add some additional material that could be of general interest.

REFERENCES

- ASA.** (1994). Industrial Cape Breton Receiving Water Study, Phase II, Vol. III, Data Report. 54 pp + 6 appendices.
- Dawson, W.B.** (1917). Tide Levels and Datum Planes in Eastern Canada from determinations by the Tidal and Current Survey up to the year 1917. Department. of the Naval Service, Ottawa, ON: 104 pp.
- Drinkwater, K., Petrie, B. & Sutcliffe, W.** (1979). Seasonal geostrophic volume transports along the Scotian Shelf. *Estuarine and Coastal Marine Science* 120(6): 4324-4339.
- Easton, A.K.** (1972). Seiches in Sydney Harbour, N. S. *Canadian Journal of Earth Sciences* 9: 857-862.
- Garrett, C.** (1972). Tidal resonance in the Bay of Fundy and Gulf of Maine. *Nature* 238: 441-443.
- Geyer, W.R. & MacCready, P.** (2014). The estuarine circulation. *Annual Review of Fluid Mechanics* 46: 175-197.
- Gregory, D., Petrie, B., Jordan, F. & Langille, P.** (1993). Oceanographic, geographic and hydrological parameters of Scotia-Fundy and southern Gulf of St. Lawrence inlets. Canadian Technical Report of Hydrography and Ocean Sciences 143. 248 pp.

- Hannah, C., Shen, Y., Loder, J. & Muschenheim, K.** (1995). Bblt – Formulation and exploratory applications of a benthic boundary layer transport model. Canadian Technical Report of Hydrography and Ocean Sciences 166. 58 pp.
- Hansen, D. & Rattray, M.** (1965). Gravitational circulation in Straits and Estuaries. *Journal of Marine Research* 23(2): 104-122.
- Hebert, D., Layton, C., Brickman, D. & Galbraith, P.S.** (2021). Physical Oceanographic Conditions on the Scotian Shelf and in the Gulf of Maine during 2020. DFO Canadian Science Advisory Secretariat Research Document 2021/070. iv + 55 p.
- Honda, K. & Dawson, W.B.** (1911). On the secondary undulations of the Canadian tides. *Science Reports of the Tôhoku Imperial University, Japan* 1: 61-66.
- Lane, P.A.** (1989). Carcinogen – circulation model for Sydney Tar Ponds. P. Lane and Associates Ltd., Halifax, N. S. Report to Supply and Services Canada, Ottawa, ON. 340 pp.
- Lane, P.A.** (1991). Analysis of Sydney Harbour Pollution Data. P. Lane and Associates Ltd., Halifax, NS. Report to Fisheries and Oceans Canada, Ottawa, ON. 154 pp.
- Miles, J. & Munk, W.** (1961). Harbor Paradox. *Journal of the Waterways and Harbors Division, Proceedings ASCE* 87: 129-130.
- Munk, W., Snodgrass, F. & Carrier, G.** (1956). Edge waves on the continental shelf. *Science* 123: 127-132.
- Okiihiro, M., Guza, R.T. & Seymour, R.J.** (1993). Excitation of Seiche Observed in a Small Harbor. *Journal of Geophysical Research* 98 (C10): 18,201-18,211.
- Petrie, B., Bugden, G., Tedford, T., Geshelin, Y. & Hannah, C.** (2001). Review of the Physical Oceanography of Sydney Harbour. Canadian Technical Report of Hydrography and Ocean Sciences 215: vii + 43 pp.
- Petrie, B. & Drinkwater, K.** (1993). Temperature and salinity variability on the Scotian Shelf and in the Gulf of Maine 1945-1990. *Journal of Geophysical Research* 98(C11): 20079-20090. doi:10.1029/93JC02191. issn: 0148-0227.
- Petrie, B., Drinkwater, K., Gregory, D., Pettipas, R. & Sandstrom, A.** (1996). Temperature and salinity atlas for the Scotian Shelf and the Gulf of Maine. Canadian Technical Report of Hydrography and Ocean Sciences 171: v + 398 pp.
- Petrie, B. & Yeats, P.** 1990. Simple models of the circulation, dissolved metals, suspended solids and nutrients in Halifax Harbour. *Water Pollution Research Journal of Canada* 25(3): 325-349.
- Smith, J.N., Lee, K., Gobeil, C. & Macdonald, R.W.** (2009). Natural rates of sediment containment of PAH, PCB and metal inventories in Sydney Harbour, NS. *Science of The Total Environment* 40: 4858-4869.
- Vandermeulen, J.H.** (1989). PAH and heavy metal pollution of the Sydney Estuary: summary and review of studies to 1987. Canadian Technical Report of Hydrography and Ocean Sciences No. 108: ix + 48 pp.

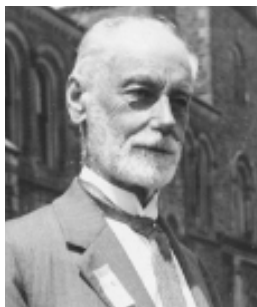


Fig A1 William Bell Dawson, engineer and superintendent of the Tidal Survey, Canadian Department of Marine and Fisheries from 1893-1924.

APPENDIX

Dr. W. Bell Dawson, born in Pictou NS in 1854, was appointed as Engineer-in-Charge of the Tidal Survey of Canada in 1893. He remained with the Survey until 1924. His appointment marked the beginning of a systematic survey of tides and currents in Canadian waters. His comprehensive program of sea level and current observations in Atlantic Canadian marine waters would lead to an improved understanding of the tides and other oceanographic phenomena in this region. The primary focus was on ports and shipping lanes.

Dr. Dawson placed considerable importance on the establishment of benchmarks and datums; these sea level reference points are particularly relevant now with the ongoing interest in rising sea levels. His publication "Tide Levels and Datum Planes in Eastern Canada, 1917" is evidence of his commitment. Dr. Dawson also carried out short period tidal observations at many secondary ports in order to establish their relationship to nearby, permanent tidal stations and enable long-term water level predictions.

Current surveys were also carried out by Dr. Dawson most notably in the Strait of Belle Isle, Cabot Strait, and at the entrances of the Bay of Fundy and the St. Lawrence Estuary. In 1894 his first current surveys were carried out in the Strait of Belle Isle and in Cabot Strait. The main objective of these programs was to quantify the currents along the routes of steamship and sailing vessels on the Atlantic coast. Consequently, the emphasis was placed on near surface (keel-depth) flows which could affect vessel movement. The report of the Belle Isle Strait survey, in particular, provides insight into the scientific mind and thoroughness that Dr. Dawson brought to his work. Dr. Dawson died in Montréal in 1944.

Dawson, W.B. (1907). *The Currents of Belle Isle Strait: From Investigations of the Tidal and Current Survey in the Seasons of 1894 and 1906*, Department of Marine and Fisheries Canada, Ottawa, ON. 43 p.

Dawson, W.B. (1917). *Tide Levels and Datum Planes in Eastern Canada: From Determinations of the Tidal and Current Survey up to the Year 1917*. Department of Naval Service, Canada, Ottawa, ON. 108 p.

Models of Honda and Dawson (1911), Easton (1972)

The harbour model of Honda and Dawson (1972) was a rectangle of constant depth, length L . Although this geometry allows for additional modes, Honda and Dawson only discuss the fundamental one. Using their harbour parameters, the next 3 modes would have frequencies of 33, 55 and 76 cpd (Northwest Arm) or 36, 60 and 84 cpd (South Arm). As noted, Honda and Dawson (1911) considered Sydney Harbour to consist of two, non-interacting parts, one from the mouth to the head of the Northwest arm, the second from the mouth to the head of the South Arm.

The one dimensional numerical model of Easton (1972) included the variations of depth and cross-section; the two arms were connected and could interact dynamically. The model dynamics were based on a balance of acceleration and along-harbour sea level gradient, and continuity. Easton (1972) shows the amplitude structure of elevation and transport of the first 4 modes. The first mode is the classic, fundamental one modified by the variations of depth and cross-section. The amplitude structure in the Northwest and South Arms are almost identical. The second mode reported appears to be associated with the South and Northwest arms only, i.e., it has a node at the junction of the south and northwest arms, whose amplitudes are 180° out of phase, and nearly zero amplitude in the outer Harbour. The third and fourth modes resemble the classic first and second harmonics again modified by depth and cross-section variations.

Determination of contribution of annual cycle to monthly mean sea level variance

Step 1 – Calculate variance by month from 15-minute datasets. Results will include contributions from periods of 30 minutes and longer (Fig 2A). Monthly variance = base value common to all months + variation above base value.

Step 2 – Determine the monthly mean sea levels to assess the magnitude of the annual cycle (Fig 2B).

Step 3 – Remove the long-term trend from the monthly sea levels to obtain the monthly residuals (Fig 2C). If the annual cycle of sea level were a pure harmonic and the only contributor, then the residuals would be 0.

Step 4 – Group the values by month from the times series shown in Fig 2C (Fig 2D).

Step 5 – Compare in Fig 2E the variation calculated from Step 1 (Fig 2A) to variance in the annual cycle (Fig 2D).

Comparison of sea level spectra from Westmount ADCP and North Sydney CHS Tide Gauge

The Westmount ADCP was equipped to detect the surface elevation relative to the instrument's position on the bottom. Sampling hourly, the record can resolve frequencies up to 12 cpd (and then only marginally)

which corresponds to the fundamental seiche mode of the Harbour. The signal can be noisy because of surface waves interfering with the acoustic backscatter. Nonetheless, between 30 Oct 2000 and 24 Apr 2001, the record of potentially 4220 points sampled hourly had only 13 missing values (3 1-hour and 5 2-hour gaps), by far the best segment of the time series. These missing values were filled using linear interpolation. During the same period, the North Sydney tide gauge (15-minute sampling) had a data gap from 13 Jan-30 Jan 2001. As a consequence of this large gap, the North Sydney record was analyzed in two segments and the results combined. Comparison of the power spectra of these data will suggest how well the Easton (1972) model captured the amplitude structure of the fundamental seiche mode in the Harbour. The model indicates that the seiche amplitude at Westmount will be about 26% larger than that at North Sydney. This is not borne out by the intercomparison (Fig A2), where the spectra suggest that the variances from 9 to 12 cpd are comparable, perhaps even larger at North Sydney. As indicated, the 1-hour ADCP sampling is not ideal to establish the relationship between the two sites.

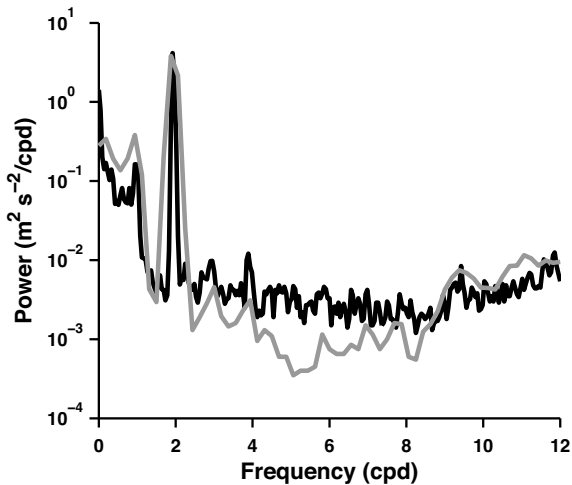


Fig A2 Spectra of the Westmount ADCP surface elevation time series (30 Oct 2000-24 Apr 2001; black line) and North Sydney sea level composite (30 Oct 2000-13 Jan 2001; 30 Jan 2001-24 Apr 2001; grey line).